Nitrogen adsorption data for the powder form of the PMO shows a diagnostic type IV isotherm with well-defined capillary condensation and very little hysteresis (Fig. 4). The Brunauer Emmett Teller (BET) surface area is found to be as high as 1706 m^2/g, and the mesopore diameter is about 2.5 nm, calculated by Barrett Joynes Halenda (BJH) methods (Fig. 4), close to that seen in TEM images (Fig. 1B). This adsorption data together with the *d* spacing of 4.7 nm given by PXRD provide an independent estimate of the channel wall thickness of about 2.2 nm, thereby corroborating the TEM-obtained diameter of the mesopores and thickness of the channel walls. Density functional theory analysis of the low pressure arm also suggests the presence of micropores with diameters in the range of 1.0 to 1.5 nm; however, further work is necessary to confirm this unambigously.

To show that the described PMO can be viewed as the parent of a whole family of mesoporous nanocomposites, we demonstrate that it is possible to lithiate the three-ring silsesquioxane precursor $[(EtO)_2Si(CH_2)]_3$ to give $[(EtO)_2Si(CHLi)][(EtO)_2Si(CH_2)]_2$ as an intermediate. We also substituted the Li^+ by electrophiles such as iodine, bromine, and iodoethane to yield the substituted three rings $[(EtO)_2Si(CHR)][(EtO)_2Si(CH_2)]_2$, (R represents I, Br, or Et). We further demonstrate that it is possible to assemble the precursors $[(EtO)_2Si(CHR)][(EtO)_2Si(CH_2)]_2$ with the use of a triblock copolymer in an acidic sodium chloride solution as the template. This assembly method was recently described by Guo *et al.* (*12*); however, a higher sodium chloride concentration was necessary in our experiments involving the substituted three-ring precursors. The obtained PMOs could be extracted with a 2 N hydrochloric acid–acetope mixture and were well ordered with a diagnostic *d* spacing of 10.1 nm for R equal to Br, 10.3 nm (I), and 10.5 nm (Et), according to PXRD (fig. S2). TEM (fig. S3) investigations corroborate this, giving additionally a pore wall thickness of about 6 nm and pore sizes of about 4.5 nm. The ^{29}Si CP MAS NMR experiments showed that no significant Si-C bond cleavage occurred during synthesis (fig. S4, A to C). The respective ^{13}C CP MAS NMR spectra (fig. S4, D to F) further indicated that the majority of the R groups (for R equal to I, Br, and Et) remained intact after synthesis and extraction, because the chemical shifts for the major signals of the ^{13}C nuclei bound to R in both the PMO and the precursor molecule are similar. The ^{13}C spectrum (fig. S4D) for the iodo-substituted ring PMO shows one signal for the CH_2 groups at 4 ppm, with a broad shoulder around –5 ppm that can be assigned to the CHI groups. Similarly, the ^{13}C spectrum for the PMO with Br as side groups (fig. S4E) shows a signal at 6 ppm for the CH_2 groups and a signal at 21 ppm that can be assigned to the CHBr units. In the spectrum for the PMO with ethyl side groups (fig. S4F), the CH_2 groups can be seen at 9 ppm, with the signals for the CHEt units appearing between 18 and 20 ppm. Furthermore, small signals around 70 ppm were observed for all ^{13}C spectra that can be attributed to the surfactant, which remained in small amounts inside the pores despite long extraction times. The small resonances at 43 and 25 ppm in the spectra S4D and S4E suggest little substitution of the halogen atoms for the bromo- and iodo-substituted ring PMOs, presumably by OH and Cl. The small signal at 21 ppm can be assigned to the CH_2 group of the surfactant's propylene blocks. To confirm this, we took a ^{13}C CP MAS NMR spectrum of the pure triblock copolymer P123, showing signals around 70 ppm for the O-CH_2-C and O-CH(CH_3)-C units of both ethylene and propylene blocks and 21 ppm for the CH_3 units of the propylene blocks. The presence of large amounts of Br and I in the respective substituted ring PMOs was also established by energy dispersive x-ray measurements, suggesting that most of the C-Br and the C-I groups are intact in the material (*13*).

References and Notes

1. K. Yamamoto, Y. Sakata, Y. Nohara, Y. Takahashi, T. Tatsumi, *Science* **300**, 470 (2003).
2. C. T. Kresge, M. Leonowicz, W. J. Roth, J. C. Vartuli, J. C. Beck, *Nature* **359**, 710 (1992).
3. T. Asefa, M. J. MacLachlan, N. Coombs, G. A. Ozin, *Nature* **402**, 867 (1999).
4. S. Inagaki, S. Guan, Y. Fukushima, T. Ohsuna, O. Terasaki, *J. Am. Chem. Soc.* **121**, 9611 (1999).
5. B. J. Melde, B. T. Holland, C. F. Blanford, A. Stein, *Chem. Mater.* **11**, 3302 (1999).
6. T. Asefa, G. A. Ozin, H. Grondey, M. Kruk, M. Jaroniec, *Stud. Surf. Sci. Catal.* **141**, 1 (2002).
7. D. J. Brondani, R. J. P. Corriu, S. El Ayoubi, J. E. Moreau, M. W. C. Man, *Tetrahedron Lett.* **34**, 2111 (1993).
8. CTMABr is cetyltrimethylammoniumbromide. The product is represented by a modified Machatschki symbol of the repeating unit $Si_3O_3(CH_2)_3$.
9. L. Dorne, N. Alikacem, R. Guidoin, M. Auger, *Magn. Reson. Med.* **34**, 548 (1995).
10. V. M. Litvinov, H. Barthel, J. Weis, *Macromolecules* **35**, 4356 (2002).
11. T. Asefa, M. J. MacLachlan, H. Grondey, N. Coombs, G. A. Ozin, *Angew. Chem. Int. Ed.* **39**, 1808 (2000).
12. W. Guo *et al.*, *Chem. Mater.* **15**, 2295 (2003).
13. The measurements for the iodo-substituted PMO revealed a weight percent ratio of Si to I of 0.63, close to the expected theoretical value for the composition $SiO(CH_2)_{0.67}(CHI)_{0.33}$ (Si/I = 0.65), whereas a weight percent ratio Si/Br = 0.88 was found for the bromo-substituted PMO, also close to the theoretical value for the composition $SiO(CH_2)_{0.67}(CHBr)_{0.33}$ (Si/Br = 1.03). Small amounts of Cl were also detected, suggesting that the Br groups became replaced by Cl to a small extent during synthesis and extraction of the PMOs in the presence of HCl. The measurements have semiquantitative character.

14. The authors thank N. Coombs for the TEM imaging and E. Xu of Micronet at University of Toronto for help with capacitance measurements. G.A.O. is a Government of Canada Research Chair in Materials Chemistry and is indebted to the Natural Sciences and Engineering Research Council of Canada for support of this work.

Supporting Online Material

www.sciencemag.org/cgi/content/full/302/5643/266/DC1
Materials and Methods
Figs. S1 to S4

26 March 2003; accepted 5 September 2003

Global Warming Trend of Mean Tropospheric Temperature Observed by Satellites

Konstantin Y. Vinnikov[1]* and Norman C. Grody[2]

We have analyzed the global tropospheric temperature for 1978 to 2002 with the use of passive microwave sounding data from the NOAA series of polar orbiters and the Earth Observing System Aqua satellite. To accurately retrieve the climatic trend, we combined the satellite data with an analytic model of temperature that contains three different time scales: a linear trend and functions that define the seasonal and diurnal cycles. Our analysis shows a trend of +0.22° to 0.26°C per 10 years, consistent with the global warming trend derived from surface meteorological stations.

For the past quarter century, passive microwave temperature soundings from the Microwave Sounding Units (MSUs) and the Advanced Microwave Sounding Units (AMSUs) on the NOAA series of polar orbiting satellites have provided vital data for both weather forecasting and climate analyses. For climate analysis, the time series of MSU channel 2 brightness temperature (temperature of radiation) measurements has been used as an indicator of air temperature in the middle troposphere. More specifically, the brightness temperature at this channel frequency is about equal to the air temperature in a broad layer centered near 500 hPa (~5.5 km). The original analyses of these data by

[1]Department of Meteorology, University of Maryland, College Park, MD 20742, USA. [2]National Oceanic and Atmospheric Administration (NOAA)–National Environmental Satellite, Data, and Information Service (NESDIS), 5200 Auth Road, Camp Spring, MD 20746, USA.

*To whom correspondence should be addressed. E-mail: kostya@atmos.umd.edu

Christy's group (*1*–*6*) indicated an insignificant global trend in the satellite-observed mean tropospheric temperature over this 25-year period, contradicting the significant warming trend retrieved from surface air temperature observations. In attempts to reconcile these findings, two separate scientific panels (*7*, *8*) have recently suggested that the apparent inconsistency may, in fact, be real and that the middle troposphere and the surface could be experiencing different temperature trends. Such a conclusion is difficult to accept, however, because it contradicts the behavior simulated by climate models (*8*, *9*).

In their papers (*1*–*6*), Christy and collaborators identified three main issues that must be addressed when using the MSU satellite observations for climate monitoring.

1) Observations from different satellites have different equator crossing times, so the data must be corrected for the diurnal cycle of temperature. Christy's group used the MSU measurements by themselves to evaluate the diurnal cycle. Unfortunately, however, the diurnal cycle cannot be validated with in situ data because of insufficient observations.

2) The MSU is a cross-track scanning radiometer, so the weighting functions and local observation time depend on beam position. Observations for beam positions other than nadir must therefore be adjusted to the observation at nadir. This problem can be circumvented through simple use of only nadir or near-nadir observations.

3) Microwave radiometers on different satellites can be biased relative to each other because of small differences in hardware and calibration errors. Christy's group proposed that these biases be estimated with the use of overlapping observations from pairs of satellites. However, it is difficult to accept their technique of correcting the MSU observations for the temporal variation of the onboard "warm target" temperature used for calibration, because the same differences in brightness temperature observed by pairs of satellites can be interpreted (partly or totally) as a manifestation of the diurnal cycle.

Nevertheless, none of the analyses performed by Christy's group (*1*–*6*) showed any significant warming trend in the satellite observations. Furthermore, even the best available subsets of global radiosonde data (*10*, *11*) are not homogeneous in time. As such, they do not provide information about the diurnal cycle of air temperature in the free atmosphere, nor can they serve as ground truth for the satellite trend estimates. Other investigators performed independent analyses of MSU data to study the climatic trend. Prabhakara and collaborators (*12*) obtained somewhat different results with the use of nadir observations, but still did not resolve the main contradictions between the MSU and surface observations. Wentz and collaborators (*13*–*15*) showed that many of the results obtained by Christy's group are reproducible even after the use of a different diurnal cycle correction based on climate model simulations. Wentz's group also used their predecessor's idea to correct the data with the use of a statistically derived linear relationship between observed brightness temperature and "warm target" temperature variations. This caused the estimated warming trend to be a little larger (and in better agreement with the trend from surface observations). Now, after more than a decade of intensive research, the satellite-based tropospheric temperature trend still disagrees significantly with the global warming trend derived from land-based meteorological stations.

To reexamine the climatic trend contained in the MSU and AMSU data, we used a technique that fits the satellite data to a model function. This approach was initially developed and validated in (*16*, *17*). It is uniquely designed for the analysis of climatic data having diurnal and seasonal cycles, with arbitrary and irregular times of observations. As such, it is particularly applicable for the analysis of multisatellite observations, each having different and changing equator crossing times.

The technique fits the MSU and AMSU measurements to a parametric model that accurately represents the expected value of brightness temperature seen from a satellite platform. This model is

$$Y(t) = A(t) + t \cdot B(t) \qquad (1)$$

where $A(t)$ represents the diurnal variations in the multiyear averages, with a fundamental period $H = 1$ day superimposed on slower annual variations with a fundamental period $T = 1$ year. The second term contains a similar function, $B(t)$, multiplied by time, t, to represent the linear trend in brightness temperature. Both functions $A(t)$ and $B(t)$ are represented by a Fourier series and given in (*18*).

The actual brightness temperature, $y(t)$, consists of the expected value, $Y(t)$, and the weather-dependent (random) anomaly, $y'(t)$, so that $y(t) = Y(t) + y'(t)$. Furthermore, $y(t)$ is different from the observed brightness temperature, $\hat{y}(t)$, because the satellite instrument introduces random noise as well as a bias, δ, which is assumed to be constant. The random noise is included in the anomaly, whereas the bias results in $y(t) = \hat{y}(t) + \delta$. Overlapping measurements from pairs of satellites are used to estimate the instrumental biases. In our analysis, the overlap periods are used to form constraints among the Fourier coefficients in Eq. 1. Each constraint equation is obtained by assuming that the anomalies of brightness temperature averaged over the overlap period of two satellites are equal, where the result is given in (*19*). Because we do not have ground truth, we must reference the biases to a common satellite instrument. This does not affect the trend estimate but only adds a constant bias to all the data. The Fourier coefficients in the model function $Y(t)$ are estimated with the use of a least squares condition that minimizes the difference between $y(t)$ and $Y(t)$ so that

$$\sum_{s=1}^{S} \sum_{t_s} [\hat{y}_s(t_s) + \delta_s - Y(t_s)]^2 = \text{minimum} \qquad (2)$$

where $\hat{y}_s(t_s)$ are the measurements for satellite s and the outer summation includes all S satellites, whereas the internal sum includes the observation times of each of satellite. The coefficients are determined by combining Eq. 2 with the constraint equations (*19*) whose number is equal to the number of satellites. Also, the number of satellite observations must be much larger than the number of unknown biases and parameters in the expression for $Y(t)$.

The complete time series (1978 to 2002) of MSU channel 2 data from nine satellites (TIROS-N, NOAA-6 to NOAA-12, and NOAA-14) and AMSU channel 5 data from four other satellites (NOAA-15 to NOAA-17 and AQUA) were used in this analysis. The data have been calibrated by NESDIS according to (*20*) and filtered for abrupt spikes related to heavy precipitation (*21*, *22*). Only the closest-to-nadir beam positions are used here. The data were preliminary averaged over 2.5° by 2.5° latitude-longitude grids and over 5-day intervals separately for ascending and descending orbits. After globally averaging these data (*23*), we obtained a time series for each of the 13 satellites, which contain

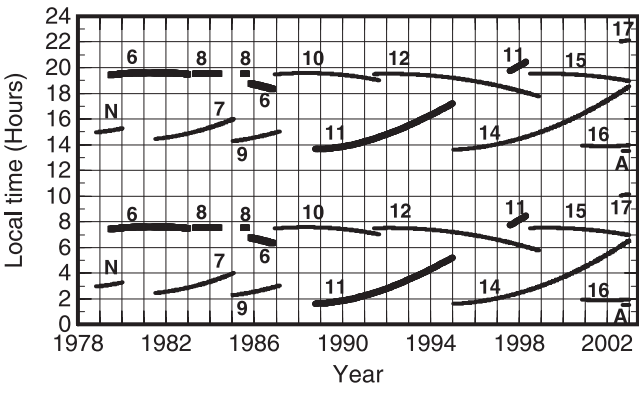

Fig. 1. Local equator-crossing time of MSU channel 2 and AMSU channel 5 on polar satellites. Line labels are the numbers of NOAA satellites; N is TIROS-N, and A is AQUA.

usually four, occasionally six, and now eight observations per day. For reference, Fig. 1 shows the local times of observation for the different satellites (*24*). Each satellite observes each location on the Earth twice a day, every 12 hours as it ascends and descends around the globe. Although the two local times are nearly fixed for a given satellite, they drift slowly during each satellite's lifetime, with some satellites having more drift than others. For technical reasons pertaining to the longevity of the satellites, observations cannot be made within a few hours around noon and midnight. Nevertheless, the existing data contain sufficient information about the first two harmonics of the diurnal cycle in $A(t)$, $K = 2$, and the first harmonic of the diurnal cycle in the trend $B(t)$, $L = 1$. To describe the seasonal variations of globally averaged temperature, we only need the two main harmonics with periods of 1 and 0.5 years. The total length of the time series is sufficient to analyze these first two harmonics in the seasonal cycle $N = 2$, $M = 2$. Incidentally, $K = 2$, $L = 1$, $N = 2$, and $M = 2$ result in a total of 40 coefficients defining $Y(t)$. The overlapping observations between satellites used in retrieving the coefficients are shown in Fig. 2. This figure also gives the length of each of the 12 overlapping periods and shows how the different satellite observations are connected to the conditionally unbiased NOAA-10 satellite.

First, we estimated the coefficients in the model and biases with the use of data only from the nine satellites containing MSU instruments. We then estimated the coefficients and biases with the use of data from all 13 satellites, which include both the MSU and AMSU instruments (bias estimates are listed in table S1). The b_{00} coefficient (*18*) in the expression for $B(t)$ is the climatic trend in annual averages of brightness temperature for the full period of observations. Interestingly, we found that the nine MSU instruments and the 13 combined MSU and AMSU instruments give the same climatic trend in brightness temperature for 1978 to 2002, which is close to 0.26 K/10 years (table S1). The error of this trend estimate is relatively small. Biases of the MSU instruments are also relatively small, less than 1 K. The larger differences in the bias between MSU and AMSU instruments are caused mostly by the small difference in frequency between MSU channel 2 and AMSU channel 5. However, it is particularly encouraging to note how small the bias variation is from one satellite to another.

The satellite-observed temporal variation of tropospheric temperature is shown in Fig. 3A: the bias-corrected (globally and pentad) averaged measurements and the derived long-term climatic trend. For comparison, Fig. 3B shows the anomaly of the satellite measurements, $y'(t)$, whose variations are random compared to the trend component. These anomalies contain fingerprints of isolated weather-related events such as El Niños and two major volcanic eruptions, which because of the long-time data record do not significantly affect the trend estimate. Figure 4 displays the seasonal and diurnal variations of the averages and linear trend of the global mean MSU channel 2 and AMSU channel 5 temperatures for the years 1978 to 2002. Seasonal variations are suppressed by global averaging but still show a prevailing signal from the Northern Hemisphere. As one would expect, the diurnal cycle has a daytime maximum and nighttime minimum. What is unexpected and contradicts what is known for land surface (*25*) is the observed diurnal cycle of the warming trend with a daytime maximum and nighttime minimum. This means that the 1978-to-2002 global warming in the troposphere has been accompanied by an increase in amplitude of the diurnal cycle, which is a contradiction of the known diurnal cycle of trends for the surface air temperature over land (*25*).

We expected that the data correction for time of observation would be important, so we ran a

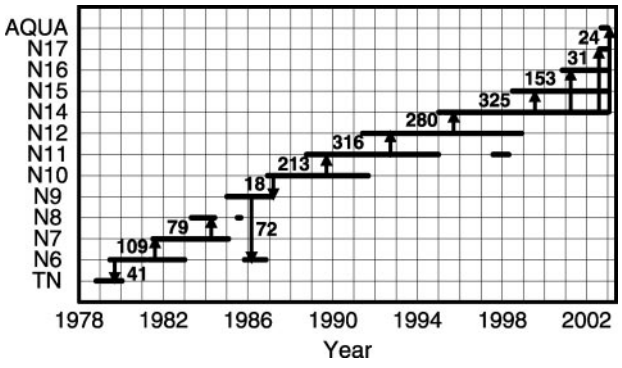

Fig. 2. Overlappings of satellite observations (in pentads) used to estimate instrumental biases from conditionally unbiased satellite NOAA-10. Connections of the satellites are shown with arrows. N, NOAA in the satellites' names; T-N, TIROS-N.

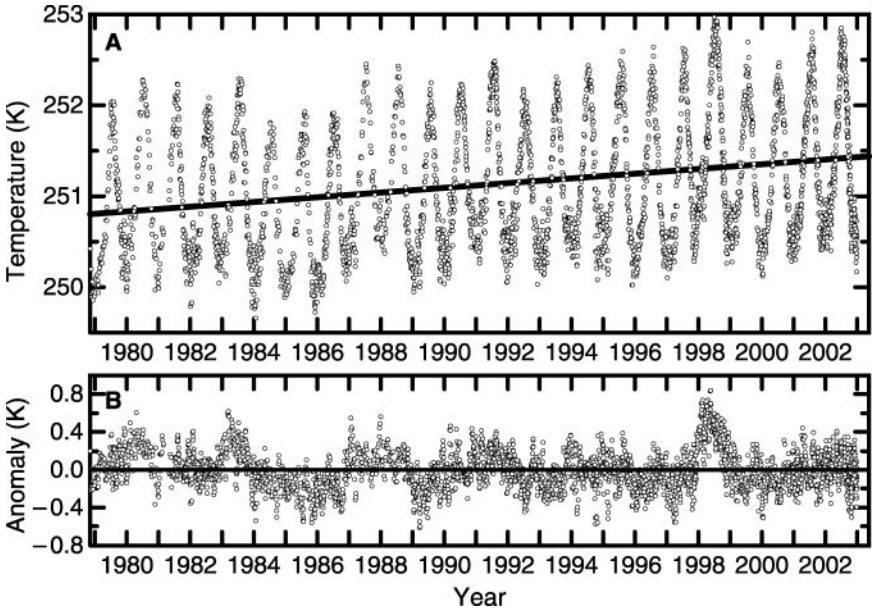

Fig. 3. (**A**) Bias-corrected globally averaged daily mean (pentad-averaged) satellite observed tropospheric temperatures (circles) and climatic trend $(a_{00} + b_{00}t)$ in annual averages (thick line). (**B**) Detrended, globally averaged daily mean (pentad averaged) anomalies, $y'(t) = y(t) - Y(t)$, of satellite observed temperature (circles).

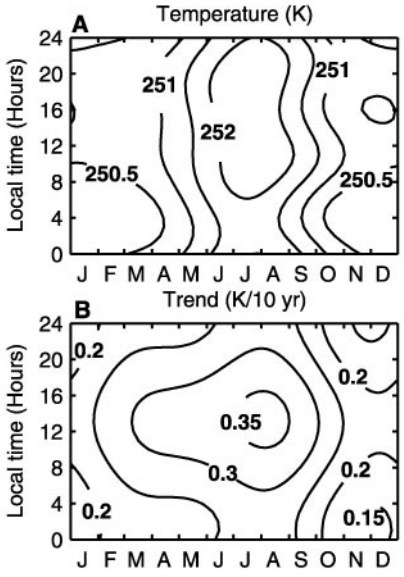

Fig. 4. (**A**) Seasonal and diurnal variations of the globally averaged 1978-to-2002 mean tropospheric temperature, $A(t)$, and (**B**) its trend, $B(t)$ (K/10 years), for the same period.

special experiment to understand how much our trend estimate depends on this correction. To do this, we assumed that the diurnal cycle is symmetric for the 12-hour intervals between satellite passes so that $K = L = 1$ in the expression for $A(t)$ and $B(t)$ in (*18*). For such a case, the averaged observations made with intervals of 12 hours give an unbiased estimate of daily averages. These estimates without the diurnal cycle correction show a global warming trend of 0.22 K/10 years. The correction for the asymmetry of the diurnal cycle increases the trend estimate to 0.26 K/10 years. This means that the real trend should not be smaller than 0.22 K/10 years. Nevertheless, the related instrument bias estimates (table S1) are contaminated by the effect of the different times of observation and are therefore less reliable than those that take into account the asymmetry of the diurnal cycle in temperature.

Our analysis systematically corrects for both the instrumental biases and different observation times of satellites. However, if one can arbitrarily neglect the effect of diurnal variation on the observations, it is possible to reduce the number of satellite instruments used in the analysis. Using $K = L = 0$ in the expression for $A(t)$ and $B(t)$ (*18*) in Eq. 1, table S4 lists the corresponding trend estimates obtained with the use of different combinations of satellite instruments. The trends vary from 0.15 to 0.36 K/10 years, where the differences are because of the errors introduced by neglecting the effects of diurnal variations on the satellite measurements. Corrections for the variation of "warm target" temperature are found to be unnecessary to be consistent with the observed trend in global surface air temperature. Furthermore, by using only near-nadir measurements, the spurious effect of decreasing satellite altitude on the weighting function is also avoided. On the basis of our analysis, the satellite estimate of the mean midtroposphere temperature trend is between 0.22 K/10 years and 0.26 K/10 years. This temperature trend is obtained by adjusting the biases of all MSU channel 2 and AMSU channel 5 measurements to that of the NOAA-10 satellite, which was conditionally considered to be unbiased. The analysis also shows that the diurnal cycle of globally averaged tropospheric temperature has an amplitude of about 0.5 K, with a maximum in the daytime that appears to be increasing with global warming at a rate of about 0.05 K/10 years.

Attempts were made to understand why our trend estimate is so different from those of our predecessors. Differences in instrument calibration can affect the results, so we first considered this as a possibility. As mentioned earlier, we used the operational data provided by NESDIS, which incorporates the latest calibration of the MSU and AMSU instruments. However, both the Christy and the Wentz groups added the same empirical adjustments to the NESDIS calibration, which are a function of the warm target temperature. But, because they both used the same calibration adjustments, one can only explain their large differences in trend (0.0 versus 0.1 K/10 years) by their different analyses. Our analytical technique of estimating the trend by simultaneously removing instrumental biases together with seasonal and diurnal variations is radically different from theirs and can possibly explain why our trend estimate is different from that of Wentz *et al*. by a factor of two. Also, as part of this investigation we found that the results of the trend analyses can depend on how the data are globally averaged. When only close-to-nadir observations are used, as in our case, part of the Earth's surface is not covered by observations. A gradually decreasing satellite altitude due to orbital decay also affects the coverage by changing both the footprint size and the number of orbits per day. However, the size of the data gaps is latitude-dependent, as is the trend itself. Because the temperature field is mostly zonal, spatial averaging must include preliminary filling of data gaps by zonally averaging the observed data or by interpolation of the data along latitudinal circles. Our analysis shows that traditional averaging algorithms that ignore gaps in the data produce significantly biased estimates of global averages, with artificial trends related to changes in the altitude of the satellites. For example, when applied to the channel 2 observations of nine MSU satellites, such averaging produces an obviously erroneous trend for 1978 to 2002 of −0.15 K/10 years. This estimate is opposite in sign to the trend that we obtained with the use of an unbiased algorithm. In our analysis of the MSU channel 2 data, we found nothing that would even remotely suggest the existence of a cooling trend in the troposphere temperature for the 1978-to-2002 period. In conclusion, generally accepted analyses (*26*–*29*) indicate that the global surface temperature is warming at a rate of 0.17 K/10 years, which is less than the estimated midtroposphere trend of 0.22 to 0.26 K/10 years obtained here. However, our analysis of satellite data confirms earlier findings based on 1959-to-1989 observations of radiosondes (*30*) and surface stations (*26*–*29*) that observed changes of globally averaged air temperature in the troposphere are at least one-third larger than temperature changes near the surface (*31*). We see good agreement between the surface and satellite observed warming trends. Our analysis also shows that the trend estimates depend on the particular connections used between instruments as well as the number of satellite observations used in the analysis.

References and Notes

1. R. W. Spencer, J. R. Christy, N. C. Grody, *J. Clim.* **3**, 1111 (1990).
2. R. W. Spencer, J. R. Christy, *Science* **247**, 1558 (1990).
3. R. C. Balling Jr., J. R. Christy, *J. Geophys. Res.* **101**, 12,827 (1996).
4. J. R. Christy, R. W. Spencer, E. S. Lobl, *J. Clim.* **11**, 2016 (1998).
5. J. R. Christy, R. W. Spencer, W. D. Braswell, *J. Atmos. Ocean. Tech.* **17**, 1153 (2000).
6. J. R. Christy, R. W. Spencer, W. B. Norris, W. D. Braswell, *J. Atmos. Ocean. Tech.* **20**, 613 (2003).
7. National Research Council, "Reconciling observations of global temperature change" (National Academies Press, Washington, DC, 2000).
8. Intergovernmental Panel on Climate Change (IPCC), *Climate Change 2001: The Scientific Basis*, J. T. Houghton *et al*., Eds. (Cambridge Univ. Press, New York, 2001).
9. S. Manabe, R. J. Stouffer, M. J. Spelman, K. Brian, *J. Clim.* **4**, 785 (1991).
10. J. R. Lanzante, S. A. Klein, D. J. Seidel, *J. Clim.* **16**, 224 (2003).
11. J. R. Lanzante, S. A. Klein, D. J. Seidel, *J. Clim.* **16**, 241 (2003).
12. C. Prabhakara, R. Iacovazzi Jr., J.-M. Yoo, G. Dalu, *Geophys. Res. Lett.* **11**, 1927 (1998).
13. F. J. Wentz, M. Schabel, *Nature* **394**, 661 (1998).
14. C. A. Mears, M. C. Schabel, F. J. Wentz, *Geophys. Res. Abstr.* **5**, 07241 (2003).
15. B. D. Santer *et al*., *Science* **300**, 1280 (2003).
16. K. Y. Vinnikov, A. Robock, D. J. Cavalieri, C. L. Parkinson, *Geophys. Res. Lett.* **29**, 10.1029/2001Gl014481 (2002).
17. K. Y. Vinnikov, A. Robock, A. Basist, *J. Geophys. Res.* **107**, 10.1029/2001JD002007 (2002).
18. $$A(t) = \sum_{k=-K}^{K} \sum_{n=-N}^{N} a_{kn} e^{i2\pi t\left(\frac{n}{T} + \frac{k}{H}\right)}$$ and $$B(t) = \sum_{l=-L}^{L} \sum_{m=-M}^{M} b_{lm} e^{i2\pi t\left(\frac{m}{T} + \frac{l}{H}\right)}$$ where the coefficients a_{kn} and b_{lm} are complex and a_{00} and b_{00} are real numbers. K and L are the number of Fourier harmonics for the diurnal cycle (period H = 1 day), whereas N and M correspond to the seasonal cycle (period T = 1 year).
19. The constraint equation for the overlapping observations of two satellites s and p is $$\delta_s = \delta_p + \langle Y(t_s) - y(t_s) \rangle - \langle Y(t_p) - y(t_p) \rangle$$ where δ_s and δ_p are instrumental biases and $\langle\ \rangle$ is the operator that averages $Y(t) - y(t)$ over all observation times t_s or t_p inside the overlap period. For the conditionally unbiased satellite (NOAA-10), we set $\delta_{\text{NOAA-10}} = 0$.
20. T. Mo, M. D. Goldberg, D. S. Crosby, *J. Geophys. Res.* **106**, 10145 (2001).
21. N. C. Grody, *J. Clim. Appl. Meteor.* **22**, 609 (1983).
22. N. C. Grody, J. Zhao, R. Ferraro, *J. Geophys. Res.* **106**, 2943 (2001).
23. Global averages for each pentad are calculated by averaging zonal mean brightness temperatures for each latitude belt with weights proportional to the area of these belts and do not include the regions within 5° of the polar caps in both hemispheres.
24. A. Ignatov, I. Laszlo, K. B. Kidwell, G. Goodrum, in preparation.
25. T. R. Karl *et al*., *Bull. Am. Meteorol. Soc.* **74**, 1007 (1993).
26. J. Hansen, R. Ruedy, J. Glascoe, M. Sato, *J. Geophys. Res.* **104**, 30997 (1999).
27. J. Hansen, R. Ruedy, M. Sato, K. Lo, *Science* **295**, 275 (2002).
28. P. D. Jones, M. New, D. E. Parker, S. Martin, I. G. Rigor, *Rev. Geophys.* **37**, 173 (1999).
29. P. D. Jones, A. Moberg, *J. Clim.* **16**, 206 (2003).
30. A. H. Oort, H. Liu, *J. Clim.* **6**, 292 (1993).
31. K. Y. Vinnikov, A. Robock, R. J. Stouffer, S. Manabe, *Geophys. Res. Lett.* **23**, 1801 (1996).

32. Sponsored by NOAA grants COMM NA17EC1483 and NAO6GPO403. The views expressed in this publication are those of the authors and do not necessarily represent those of NOAA. We thank M. D. Goldberg for recommending this study; A. Robock, R, Stouffer, A. Kagan, M. Weinreb, G. Ohring, D. Tarpley, I. Laszlo, A. Ignatov, J. Sullivan, S. Grodsky, R. Etkins, and N. Kovyneva for their useful comments and discussions; and Z. Chang for initial processing of the satellite data.

Supporting Online Material

www.sciencemag.org/cgi/content/full/1087910/DC1
Tables S1 to S4

11 June 2003; accepted 3 September 2003
Published online 11 September 2003;
10.1126/science.1087910
Include this information when citing this paper.